Experimental Study of Composition Variation During Flow of Gas-Condensate

Hai X. Vo, and Roland N. Horne, Stanford University

Abstract

A significant and unique factor associated with gas-condensate reservoirs is a prominent decrease in productivity once the flowing bottom-hole pressure drops below the dew-point pressure. Gas-condensate reservoirs exhibit complex phase and flow behaviors due to the appearance of a condensate bank in the near-well region, and differ in their behavior from conventional gas reservoirs, especially for low permeability, high-yield systems where the condensate banking is more severe.

However, there is still a lack of understanding phase and flow behaviors of gas-condensate reservoirs. The difficulty lies in the variation of the composition of the in-situ fluid due to the accumulation of heavy components in the condensate phase. A good understanding of how the gas condensate reservoirs vary in composition is very important to optimize the producing strategy, to reduce the impact of condensate banking, and to improve the ultimate gas recovery.

The composition variation has been observed in the field but its effects have been reported rarely in the literature. This work studied compositional variation of gas-condensate systems through a series of laboratory experiments and supporting numerical simulations. The study verified claims on the effect of flow through porous media on the apparent behavior of a gas-condensate mixture. These include compositional variation during depletion, failure to achieve condensate revaporization upon well shut-in, and the effect of well bottom-hole pressures on condensate banking. The effect of irreducible water saturation on the composition variation was also studied.

Results from this study show that composition can vary significantly during depletion. Due to the difference in mobilities and accumulation effect, the composition of the mixture will change locally. The overall composition near the wellbore becomes richer in heavy components. As a result, the phase envelope of fluid will shift. Near-well fluids can undergo a transition from retrograde gas to volatile oil. By taking account of the new understanding of the impact of compositional changes, the liquid dropout can be "controlled" by the production strategy. Also, some common practices, for example shutting wells after condensate drops out to revaporize the condensate can be understood to be ineffective.

Introduction

Gas-condensate reservoirs are encountered frequently. The gas condensate usually consists mainly of methane and other light hydrocarbons plus a small portion of heavier components.

Gas condensate has a phase diagram as in Fig. 1. In this case, reservoir temperature lies between the critical temperature and the cricondentherm, the maximum temperature at which two phases can coexist in equilibrium. Initially, reservoir pressure is at a point that is above the dew-point curve so the reservoir is in the gaseous state only. During production, the pressure declines isothermally from the reservoir boundary to the well. If the flowing bottom-hole pressure (BHP) of the well drops below the dew-point pressure p_d, the condensate drops out of the gas and forms a bank of liquid around the well (Fig. 2).
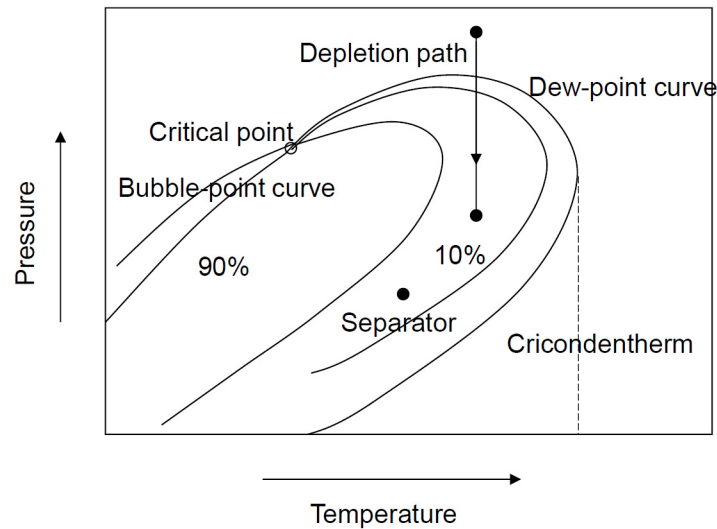
Figure 1—Phase diagram of a typical gas condensate with line of isothermal reduction of reservoir pressure.
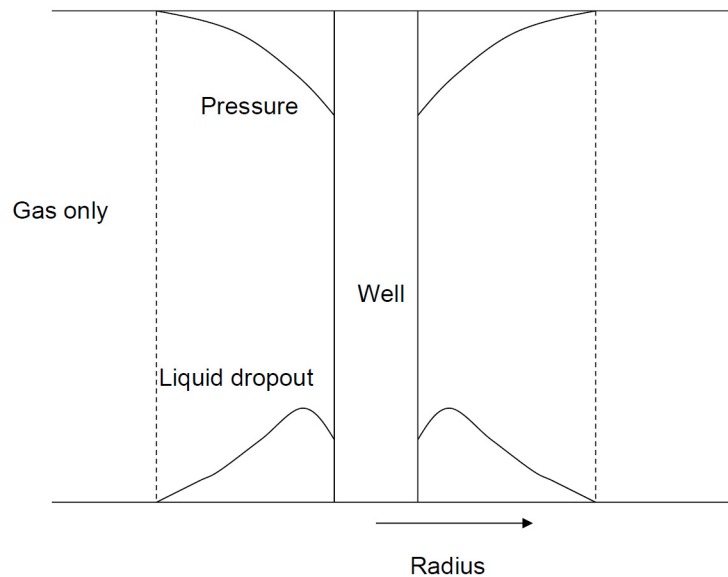
Figure 2—Illustration of pressure profile and liquid dropout in the near wellbore region.

When the condensate drops out in the reservoir, at first, due to relative permeability effects, the condensate liquid will not flow until the accumulated condensate exceeds the immobile liquid saturation. This leads to a loss of valuable hydrocarbons because the condensate contains most of the heavy components. Besides that, near the wellbore where the condensate bank appears, the gas relative permeability is reduced. The reduction of gas permeability due to the condensate bank is called condensate blocking. The condensate blocking leads to a reduction of gas productivity of the well.

The gas productivity loss due to condensate buildup is large in some cases, especially in tight reservoirs. Afidick et al. (1994) reported that liquid accumulation had occurred around the wellbore in the Arun field and that it had reduced individual well gas productivity by 50% even though the retrograde-liquid condensation in laboratory Pressure-Volume-Temperature (PVT) experiments was about 1.1% of the pore volume. Barnum et al. (1995) conducted a study using data from 17 fields and concluded that the condensation of hydrocarbon liquids in gas-condensate reservoirs can restrict gas productivity severely. Notably, gas recovery factors below 50% were found more often in low permeability reservoirs (with a permeability-thickness less than 1,000 md-ft). For more permeable reservoirs, the productivity loss was not very severe.

The study of productivity loss in gas-condensate wells started back in the 1930s but due to the complex phase and flow behaviors, it is still an outstanding problem. The problem of condensate banking was addressed early on by Muskat (1949) in his discussion of gas cycling. Muskat estimated the radius of the condensate blockage as a function of time, gas rate, rock and fluid properties. Kniazeff and Naville (1965), and Eilerts et al. (1965) independently developed numerical models to estimate the saturation and pressure in the vicinity of the wellbore. Later, O'Dell and Miller (1967) presented a method for calculating the volume of retrograde liquid around the producing wellbore and its effect on the producing rate based on the steady-state flow concept. Roebuck et al. (1968a, 1968b) developed the first models for individual component flow and considered the component mass transfer between phases. Fussell (1973) used a modified version of the models developed by Roebuck et al. and concluded that the productivity of the well could be reduced by a factor of three compared to that predicted by the method of O'Dell and Miller due to condensate accumulation in the region around the producing well. Jones et al. (1986), and Jones and Raghavan (1988) analyzed the pressure transient response, steady-state flow and placed modification of the relation given by Fussell for a gas-condensate system using compositional simulation. Fevang and Whitson (1996) addressed the physics of the condensate banking and proposed a generalized analytical well deliverability model based on the concepts developed earlier by Muskat, O'Dell and Miller, Jones et al..

The difficulty of understanding the phase and flow behaviors lies in the compositional variation of the fluid in situ. Novosad (1996) and Roussennac (2001) used compositional simulation and proved that near-well fluids can undergo transition from retrograde gas to a volatile oil early in the depletion, passing through a critical composition in the process if the BHP of the well drops below the dew-point pressure. Due to the condensate drop out and condensate accumulation plus difference in mobilities of the gas and condensate phases, the composition of the fluid will change locally. The overall composition near the wellbore becomes richer in heavy components. As a result, the phase envelope will shift to the right and the fluid behavior changes from initial gas-condensate to volatile oil. This brings a large change in phase properties and saturation, and thus flow behavior. El-Banbi and McCain (2000) stated that composition change due to condensate dropout will affect the surface tension and viscosity of the fluids. These effects will impact the mobilities and hence productivity. A theoretical model was also developed by Zhang and Wheaton (2000) to understand the condensate banking dynamics. The model shows that during production, around the well, composition varies as what is observed in the numerical simulation.

Enhancing the recovery of gas condensate reservoir has also been an active research area. Shi et al. (2006) addressed issues related to the behavior of the composition variation, condensate saturation buildup and condensate recovery during the gas-condensate producing process. Shi and Horne (2008) investigated optimum producing strategy when the well is brought into production to reduce the productivity loss caused by the condensate banking effect. Seah et al. (2014) addressed the effectiveness of different production methods and remediation solutions in minimizing condensate buildup below the dew-point pressure. Izuwa et al. (2014) investigated a range of production strategies in gas cycling project using the predictive model to assess the effects of the reservoir and production parameters on recovery of gas and

condensate. Siddiqui at al. (2014, 2015) applied stochastic optimization algorithms to find optimal well placement and gas cycling operational parameters.

Despite some numerical and theoretical studies, the compositional variation during flow that affect phase and flow behaviors has not been sufficiently studied through direct experiments. Shi et al. (2006), Shi and Horne (2008), Shi (2009), Vo (2010), and Al Ismail and Horne (2014) reported investigations on compositional variation during flow of the gas-condensate system through laboratory core flood experiments in the absence of immobile water. The ultimate objective of the work described in this paper was first to demonstrate repeatability of the results from experiments performed by Shi. Furthermore, we expanded the study in other experiments to understand other phenomena. For example, the work was extended to the case that we normally see in the field, namely gas-condensate reservoirs where immobile water is present.

Experimental Investigation

Experimental Design

Synthetic Gas-Condensate Mixture   The strategy in the experiments was to use a simple binary mixture. Although field gases have more complex composition, the use of a binary mixture in the laboratory improved the ability to achieve accurate results. The laboratory results obtained using the binary mixture could then be used subsequently to confirm numerical simulation results with the same composition.

The binary mixture used in the experiments was 85% methane (C_1) and 15% n-butane (nC_4) by mole fraction. This gas-condensate mixture was selected based on the following criteria:

- The binary mixture is easy to mix in the laboratory, from commercial pure component gases.
- The critical temperature T_c of the mixture is below the laboratory temperature so the experiments can be performed at room temperature, which eliminates the need to heat the flammable gases hence improving safety.
- The gas has a broad two-phase region which makes it easier to achieve condensate dropout during the experiment.

The phase diagram of the synthetic gas-condensate mixture used for the experiments is shown in Fig. 3. The critical point of the mixture is T_c= 10 °F, critical pressure p_c= 1,844 psia. At room temperature of 70°F and pressure range from 2,200 down to 1,000 psia, this mixture has a broad two-phase region.
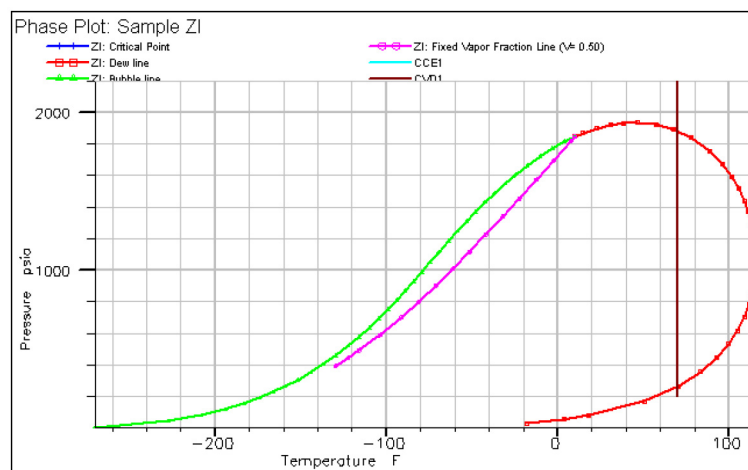
Figure 3—Phase diagram of the synthetic gas-condensate mixture used for experiments (85% C_1 and 15% nC_4 in mole fraction).

Fig. 4 shows the condensate dropout volumes in Constant Volume Depletion (CVD) and Constant Composition Expansion (CCE) tests. The accumulated condensate volumes from both tests are similar in the condensing region. Both tests also show that the condensate revaporizes into the gas phase at lower pressure. These static PVT tests do not account for the condensate accumulation hence they do not indicate the maximum possible condensate in the reservoir. The maximum liquid dropout volumes from these simple PVT tests are less than 10%. However, as we found from reservoir simulation (shown later), the condensate saturation during actual flow of this mixture can be as high as 47% due to condensate accumulation.
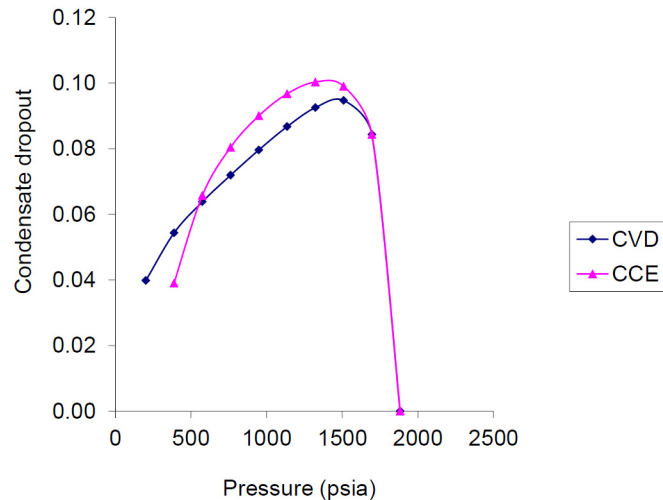
Figure 4—Condensate dropout of the synthetic gas-condensate mixture used for experiments at 70 °F from CCE and CVD tests.

Numerical Simulation for Experiments   The core used for experiment is low permeability sandstone (Fig. 5a). The synthetic gas-condensate mixture is injected at one end and exits the other end of the core, so the flow is one-dimensional linear flow. The simulation for this linear flow can be done in a one-dimensional Cartesian coordinate system (Fig. 5b). The core is divided into 51 grid blocks in the x-direction only. The cross-section of the grid block is a square whose area is equal to the cross-sectional area of the cylindrical core. The reason to do so is to maintain the same pore volume.

(a) Core used for experiments   (b) Gridding for numerical simulation

Figure 5—Numerical simulations of core flooding experiment.

Numerical simulations were conducted in this study to define the experimental parameters such as time duration. Simulation was also used to check the flow pressures and to have an idea how composition and

saturation were distributed along the core. In the simulation model, two wells, one gas injection and one producing, were used. Both wells were controlled by constant bottom-hole pressures. The bottom-hole pressure of the injection well was set above the dew-point pressure while the bottom-hole pressure of the producing well was set below the dew-point pressure of the gas-condensate mixture. So the fluid at the upstream end was always in the gas phase, and the fluid at the downstream end was always in the two-phase region.

First, simulation for a two-phase gas-condensate system was performed. Based on the phase diagram in Fig. 3, we set the bottom-hole pressure for the injection well at 130 atm (1,911 psi) and for the producing well at 70 atm (1,029 psi). Fig. 6a shows that liquid saturation builds up quickly once the pressure drops below the dew-point pressure. After two minutes the system reaches steady state (curves do not change versus time). Hence if the experiments last three minutes, the flow will be stable and gas samples taken will be representative. It is also shown in Fig. 6a that the maximum condensate accumulation at the steady state can be as high as 47% whereas the maximum liquid dropout from the CCE and CVD experiments are only about 9%. This is because the numerical simulation takes into account the condensate accumulation due to relative permeability effects. Obviously, the liquid saturation at the upstream end will be zero as the upstream pressure was still above the dew-point pressure. As shown in Fig. 6b, the nC_4 compositions in the vapor phase change dramatically along the core (pressure drop is higher on the right) once the condensate has dropped out. The vapor phase becomes lighter hence the concentration of nC_4 in the vapor phase decreases in the direction of flow.

(a) Condensate saturation profile   (b) nC_4 mole fraction in the vapor phase
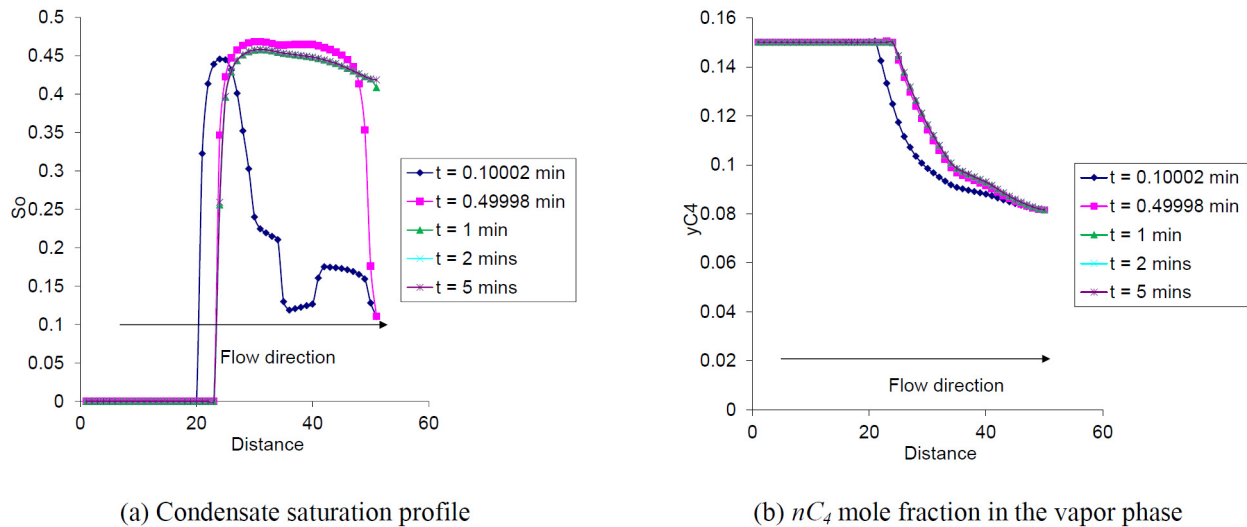
Figure 6—Two-phase (gas–condensate) simulation.

We extended the simulation study to investigate gas condensate flowing through a core in the presence of immobile water. The segregation model in Eclipse was used for the oil relative permeability. The mutual solubilities of water and hydrocarbons are small, so to simplify the problem the hydrocarbon phase behavior can be studied independently of the water phase. Nevertheless, to model the water-hydrocarbon compositional effects properly (assuming any exist because of initial nonequilibrium of injected mixture and connate water), we would need to use a simulator that uses a nontraditional (non-van der Waals) mixing rule.

Using this assumption, first we wanted to check our three-phase model by setting the immobile water saturation S_{wi} to zero and comparing the results with the results from the two-phase case. Fig. 7 shows that the results of three-phase system with $S_{wi} = 0$ are the same as the results of two-phase system (Fig. 6). This demonstrated that the three-phase model for simulation was consistent.

(a) Condensate saturation profile   (b) nC$_4$ mole fraction in the vapor phase
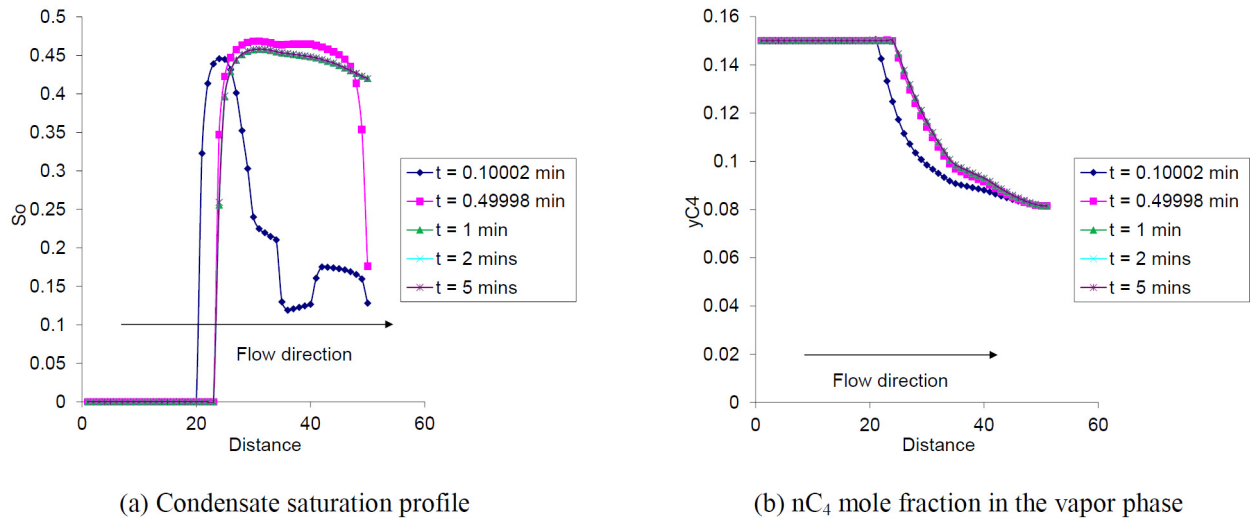
Figure 7—Three-phase simulation result with S_{wi} = 0.

The simulation results for the gas-condensate mixture flowing in the presence of immobile water (S_{wi} = 0.16) are shown in Fig. 8. As we can see, there is some difference in composition between the three-phase system (gas-condensate-immobile water) and the two-phase system (Fig. 6) during the transient period. However, after the flow reaches steady state, the composition is the same for both systems.

(a) Condensate saturation profile   (b) nC$_4$ mole fraction in the vapor phase
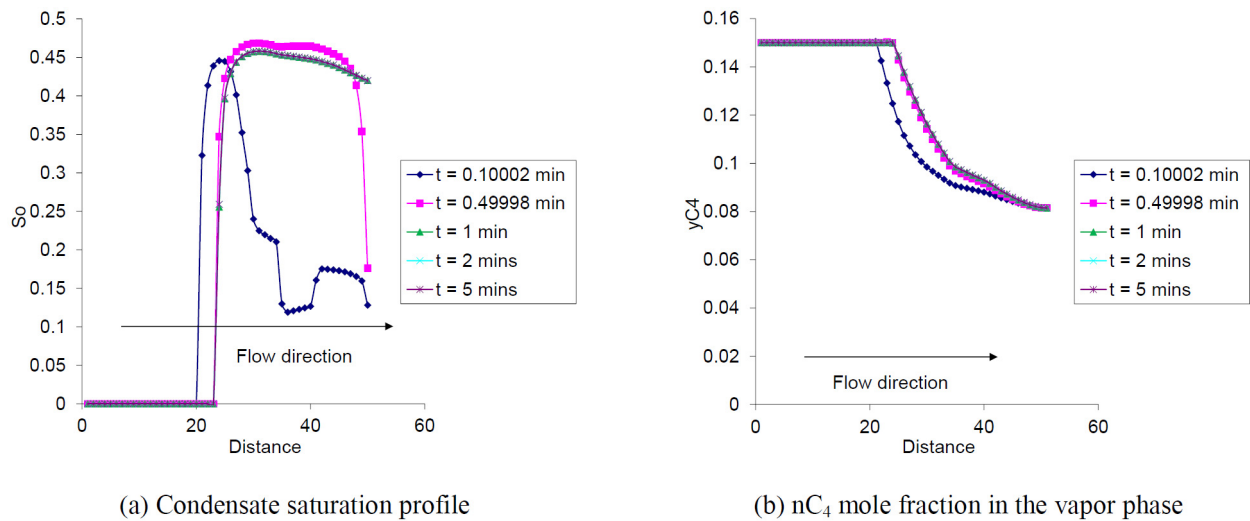
Figure 8—Three- phase simulation result with S_{wi} = 0.16.

Experimental Apparatus

The core-flooding apparatus was modified from the previous design of Shi and Horne (Shi et al. 2006, Shi and Horne 2008, Shi 2009) to seek repeatability of the experimental results. The modified design is shown in Fig. 9. The modified experimental apparatus consists of the three main subsystems: gas supply and exhaust, core flooding system and fluid sampling system.
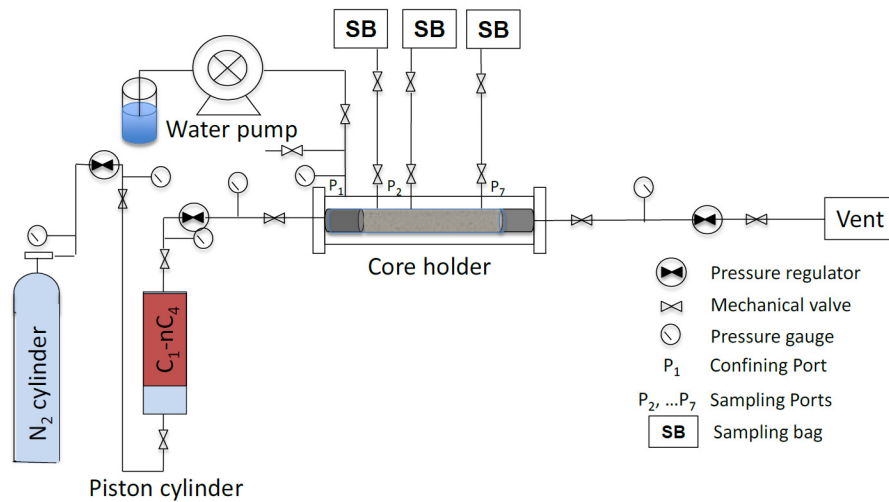
Figure 9—Experimental apparatus.

Gas Supply and Exhaust

The synthetic gas-condensate mixture was mixed in a piston cylinder. This piston cylinder has an internal volume of 3,920 ml and pressure rating of 4,641 psi. During the experiments, the pressure of the gas mixture was maintained about 200 psi above its dew-point pressure by pushing the back of the piston using a 6,000 psi N_2 driving-gas bottle. O-rings in the piston prevent the gases on both sides from mixing together hence a high constant pressure gas mixture supply is achieved without affecting the gas composition. Two types of experiments were conducted: capture and noncapture. During the noncapture experiments, the downstream gas was discharged directly to the ventilated cabinet because the volume of exhaust gas is small. During the capture experiments or during noncapture experiments in the computerized tomography (CT) scanner room (where the ventilated cabinet was not available), the exhaust gas was discharged into an empty piston cylinder.

Core Flooding System

The core flooding system consists of a titanium core holder, Berea sandstone core plug, valves and pressure regulators. The core holder can support a maximum confining pressure of 5,800 psi while maintaining the pore pressure at 5,366 psi. Application of confining pressure was performed through port P_1. There were six ports (P_2 to P_7) to allow pressure monitoring and fluid sampling, but these ports were modified to fit shut-off valves. Adding the valves directly on onto the core holder minimizes the dead volumes. In the previous design, the dead volume was big so samples taken during flow were contaminated by the residual gas.

These and other hardware modifications allowed us to achieve repeatable results, as will be discussed in the **Results and Discussion** section. The core used in this work is Berea sandstone used previously by Shi and Horne. The Berea sandstone core has a length of 30 cm and diameter of 4.9 cm. The permeability of the core is 9 md and its porosity is 16%. Upstream and downstream pressures were regulated using a pressure regulator and a back-pressure regulator.

Fluid Sampling System

One of the key modifications to achieve repeatability in the experiments was to make sure that the whole volume of gas sample captured at each port during the experiments was transferred completely to the plastic bag. This is because if the volume of the gas sample captured is bigger than the volume of the plastic bag, when we transfer the gas the pressure drops below the dew point and condensate drops out in the sampling tubing. However, gas is moving faster than the condensate so the gas in the plastic bag may not be the same as the captured gas in term of composition. For this reason, a 0.4 m long tubing,

which has smaller volume than the volume of the plastic bag, was connected to the valve on each port. The other end of the tubing was fitted with another valve. Before taking samples, the tubing was vacuumed and the valves were closed. A sample was taken by opening the valve on the core holder, waiting for 30 seconds and closing it. The sample could be then transferred to the plastic sample bag. The pressure transducers were not connected to the tubing during this work to simplify the hardware configuration.

Compositional Measurement

The gas chromatograph (GC) used for this study was an Agilent 3000 Micro GC. Before being used for compositional analysis, the GC was calibrated. Calibration is the process of relating detector response to the amount of material that produces that response by analyzing specially prepared calibration mixtures with known concentrations. Response factors calculated from the calibration are then used to convert the detector response area to the concentration to the gas mixture that needs to be analyzed. Calibration is also used for peak identification. As the gas mixture we analyzed consists of around 85% C_1 and 15% nC_4 in moles, a gas mixture standard with the mole composition of 85%-15% C_1-nC_4 was used to calibrate the GC. A single-level calibration and linear calibration curve fitting are sufficient. C_1 is detected in detector 1 (Molecular Sieve type) and nC_4 is detected in detector 2 (PLOT type). After being calibrated, the GC is ready to analyze the composition of gas samples taken during the experiments. A typical gas chromatogram of the samples is shown in Fig. 10.
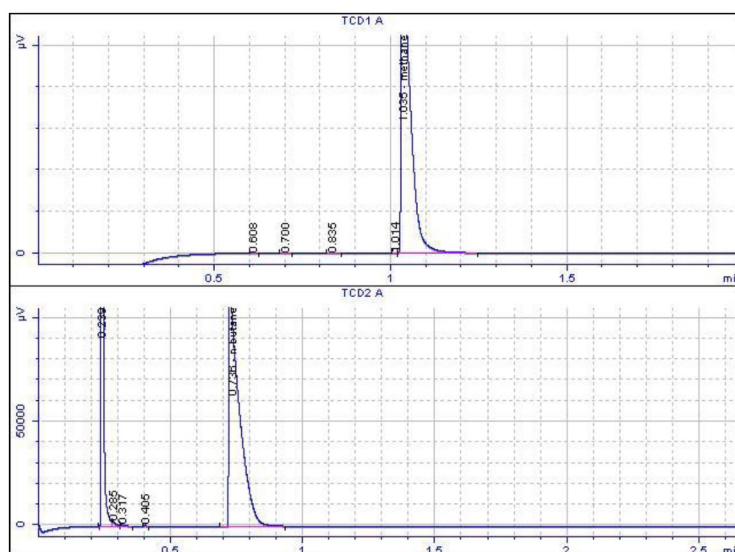
Figure 10—A typical gas chromatogram of gas samples taken during experiments.

Saturation Measurement

In this study, a Computerized Tomography (CT) scanner was used to measure the saturation distribution along the core during the experiments (Fig. 11). For two-phase systems and three-phase systems where the third phase is immobile, a single energy level scan is sufficient to determine the saturations. The condensate saturation (S_o) is calculated using Eq. 1

Figure 11—Performing experiments in the CT scanning room.

$$S_o = \frac{CT_{exp} - CT_{gr}}{CT_{cr} - CT_{gr}}$$ (1)

where the subscripts *exp, gr* and *cr* represent the *CT* number of the rock during the experiment with the C_1-nC_4 mixture, C_1-saturated, and nC_4-saturated rock, respectively. The scanning slices were chosen carefully to be located between the sample ports. Table 1 shows scanning locations. The tubing and plastic valve handles were removed to make sure the scanning slices were clear of any obstruction to achieve the best result possible. Slice #1 is on the upstream of the confining-pressure port P_1 (from upstream edge), slice #2 is between P_1 and sampling port P_2, etc., and slice #8 is on the downstream of last port P_7.

Table 1—Scanning locations for saturation measurement.

Slice	Distance from the upstream edge of the core holder (mm)	Thickness of the slice (mm)
1	118	3
2	158	3
3	198	3
4	238	3
5	278	3
6	318	3
7	358	3
8	370	3

Experimental Procedures

Gas-condensate Core Flooding Experiments   Two types of experiments were performed in this study: noncapture and capture. The difference between them was that in the noncapture experiments the samples were taken while the fluid was flowing, while in the capture experiments samples were taken from the "captured" fluid after flowing it through the core for a given time period then closing both inlet and outlet valves at the same time. At the end of capture experiment, the remaining fluid in the core was discharged to an empty cylinder to determine the composition of the condensate left in the core. These experimental

procedures were modified from the previous procedures of Shi and Horne to achieve repeatability of the results.

In both type of experiments, the whole system was vacuumed overnight and the core was presaturated with C_1 at 2,200 psi. This was done to make sure that the gas-condensate mixture was in the gaseous state in the core and we could flush the gas mixture through to core to displace methane without dropping below the dew-point pressure of the gas mixture. The gas-condensate cylinder was compressed to 2,200 psi (dew-point pressure of the 85%-15% moles C_1-nC_4 is around 1,840 psi) using N_2 pushing on the back of the piston inside the cylinder. The gas-condensate mixture was flushed through the core for 10 minutes with the downstream pressure at 2,000 psi (160 psi above the dew-point pressure of the gas mixture). Then the downstream valve was closed and the fluids were sampled under no-flow conditions. The first five batches of samples were discarded to eliminate all residual methane in the dead volumes of the sampling ports. The sample tubing was vacuumed and no-flow samples were then taken. After demonstrating good repeatability under no-flow conditions, the sample tubing was vacuumed again. The gas-condensate mixture was then flowed through the core at 1,000 psi differential pressure for 3 minutes.

In the noncapture experiments, flow samples were taken during flow. Then both upstream and downstream valves were then closed and the core flooding system was detached for CT scanning. To avoid artifacts in X-ray CT images, the sample tubing was removed before scanning. The plastic handles of the valves on the core holder were also removed. The core was then scanned by the X-ray CT scanner to determine the saturation distribution.

The compositional behavior under different well flowing bottom-hole pressure (BHP) control was then investigated using the noncapture experiments. The experimental procedure was to keep the upstream pressure fixed but vary the downstream pressure and measure the composition corresponding to each downstream pressure.

We also studied the effect of pressurization on revaporization of the condensate during noncapture experiments. The procedure of the pressurization experiment was to first perform all the above steps for the noncapture experiment. After taking the flow samples, we shut the downstream valve and let the pressure in the core build up to 2,200 psi. After about 35 to 40 minutes, samples along the core were taken. This procedure mimics the real situation in which a well is producing in a gas-condensate reservoir: after the BHP drops below the dew-point pressure, and the well is shut in in an attempt to achieve condensate revaporization.

Capture experiments were designed to have samples under conditions in which both upstream and downstream valves were closed so the samples would be closer to static composition rather than that of the flowing gas. Furthermore, the captured condensate in the core could be discharged to an empty cylinder to determine the composition of the condensate dropout. In this experiment, instead of taking samples at flow condition, both upstream and downstream valves were closed simultaneously. Fluid samples were then taken in capture mode immediately. At the end, the entire content of the core was discharged into an empty (vacuumed) cylinder for compositional analysis.

Gas-Condensate Core Flooding in the Presence of Immobile Water Experiments First, the core holder was vacuumed (about 48 hours if there was some water in the core previously). The vacuum pump was connected at the outlet of the core holder through a transparent tubing, the inlet valve was closed. Second, the core is saturated with water. This is done by connecting the water pump to the inlet of the core holder and pumping the deionized (DI) water through the core while keeping the vacuum pump on. The vacuum pump was turned off and disconnected when water reached the transparent tubing at the outlet of the core holder. The estimated time was calculated based on the water pumping rate and the pore volume. Water pumping was continued to displace about four pore volumes to eliminate any air trapped in the core. Next, the water in the core is drained to immobile water saturation. The procedure is to lift the upstream of the core to an angle about 30 degrees from horizontal. C_1 was injected through the core at 50-100 psi

for two to three hours to drain the water to immobile water saturation S_{wi}. The sample tubing was also bled off from time to time to release trapped water. Finally, the core holder was then put back to the horizontal position, the downstream valve was closed and the core was filled with C_1 at 2,200 psi. The capture and noncapture experiments were performed using the same procedures as for the gas-condensate system. Note that no CT scanning was performed during the gas-condensate-immobile water experiments.

Results and Discussion

Compositional Variation in Gas-Condensate Flow

Noncapture Experiments The compositional distribution along the core during a gas-condensate non-capture experiment is shown in Fig. 12a. No-flow samples were taken before the flow test when the gas mixture was above the dew-point. The no-flow compositions were repeated exactly and were identical to the composition from the source cylinder. This indicated that the rock does not have an effect on the (static) phase behavior of the gas mixture.
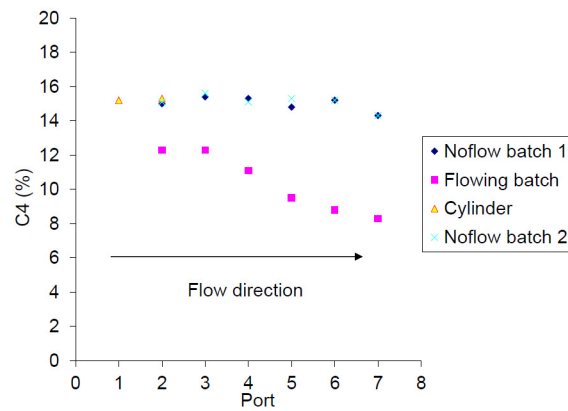
(a) Experiment 1
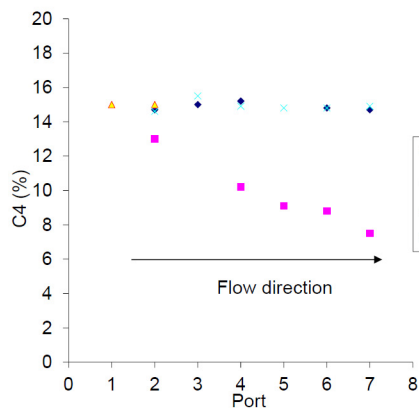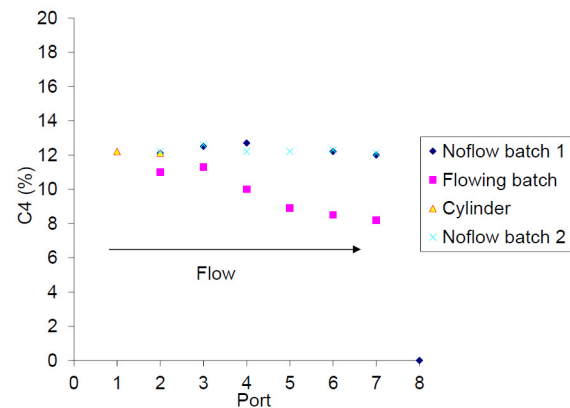
(b) Experiment 2   (c) Experiment 3

Figure 12—Mole fraction of C_4 in the following mixture during noncapture experiments.

During flow through the core, going from left to right, the pressure drop was higher on the right. Liquid dropped out and accumulated in the rock. The flowing mixture became lighter (more C_1) and the concentration of nC_4 in the flowing phase along the core decreased.

Figs. 12b and 12c show results of two additional noncapture experiments following the same procedure. The compositional distributions along the core have the same trend as Fig. 12a. These results also confirm the simulations results in Fig. 6.

The effect of producing pressure (BHP in a real well) on the composition is shown in Fig. 13. The result in Fig. 13 shows that the higher the pressure drop below the dew-point the more nC_4 accumulates in the condensate and the less nC_4 is found in the flowing mixture. The experimental result in Fig. 13 also confirms the simulation results shown by Shi and Horne (2006). This finding is important because it provides us a way to minimize the condensate dropout by minimizing the pressure drop below the dew-point by either producing the well at higher pressure or applying pressure maintenance.
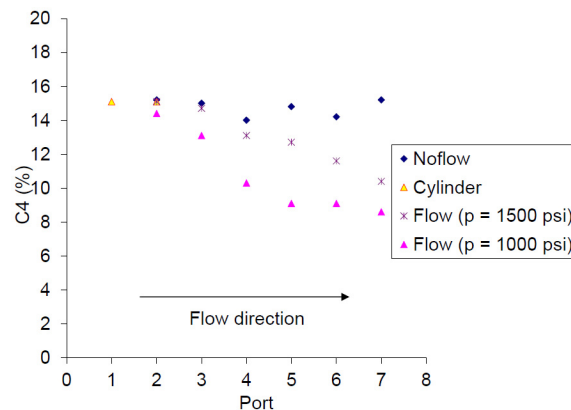
Figure 13—Effect of BHP on composition of C_4 in the following mixture during noncapture experiments.

Fig. 14 shows effect of pressurization on revaporization of the condensate during noncapture experiments. In the first experiment (Fig. 14a), composition during flow was not registered. However in the other two experiments (Figs. 14b and 14c) it is clear that the composition changes after pressurization, but not all the way back to the original gas composition after about 35 to 40 minutes of shutting valves. This confirms shift of the phase envelope from the numerical simulation (Fig. 15). Hence shutting the well may not be an effective strategy to remove the condensate bank.
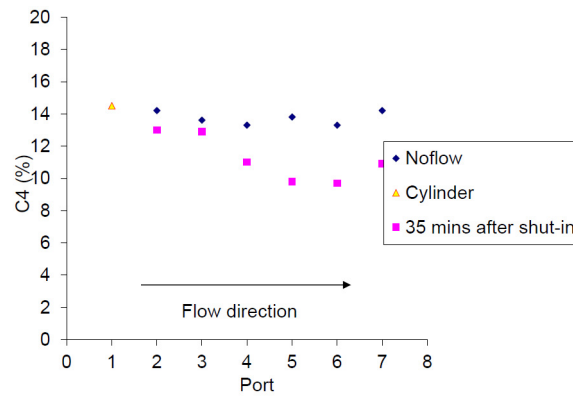
(a) Experiment 1
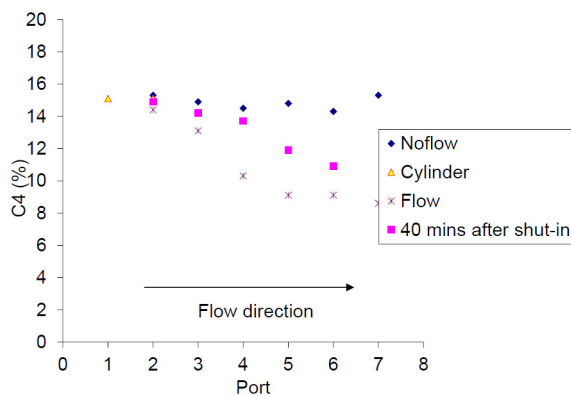
(b) Experiment 2
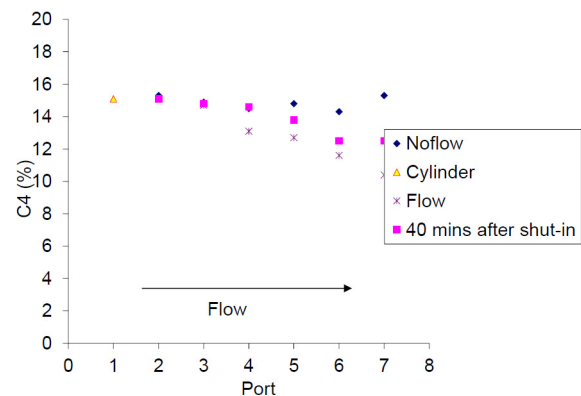
(c) Experiment 3

Figure 14—Effect of pressurization on revaporization of the condensate during noncapture experiments.
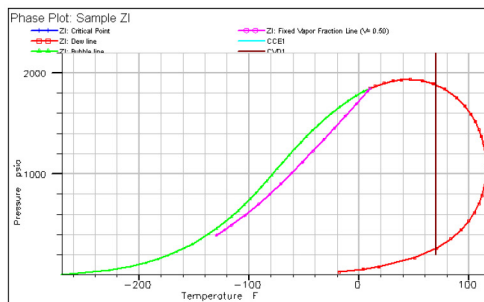
(a) Original phase envelope
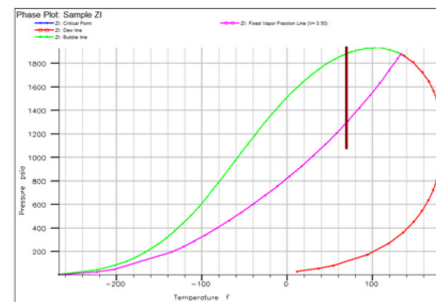
(b) Phase envelope after condensate dropout

Figure 15—Conversion of gas-condensate system to volatile oil system in the last gridblock (#51).

Capture Experiments The results of a capture experiment are shown in Fig. 16a. Good repeatability was achieved under both static conditions and flowing conditions. The compositional distribution along the core shows a similar trend of liquid dropout as noncapture experiments. A second capture experiment (Fig. 16b) confirmed the result of the first capture experiment. Fig. 16c shows the result of another capture experiment. However in this case, after taking samples in the capture mode, we discharged all gas and condensate into a vacuumed empty cylinder. When the core and discharge cylinder reached pressure

equilibrium (at low pressure), we disconnected the core from the cylinder and took samples from each of them. The nC_4 compositions in the discharge cylinder and core were very high, which confirmed that the liquid condensate had deposited in the core.
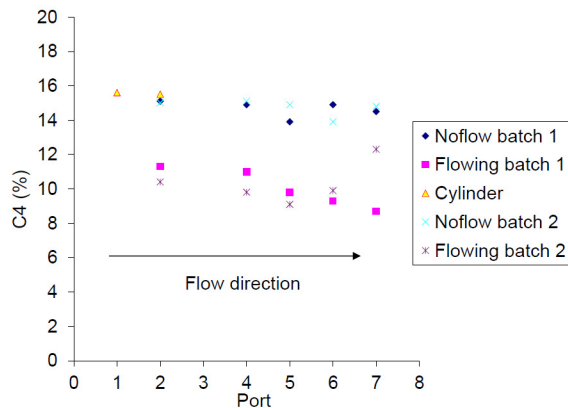
(a) Experiment 1
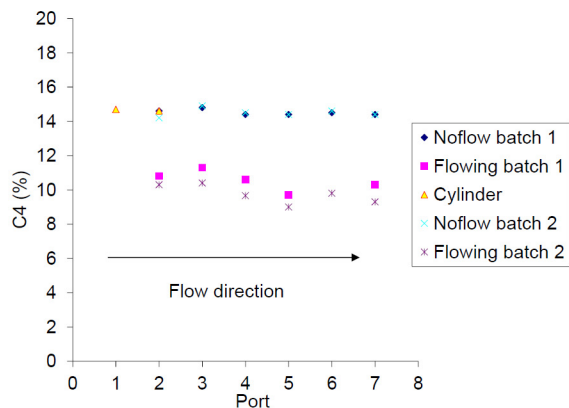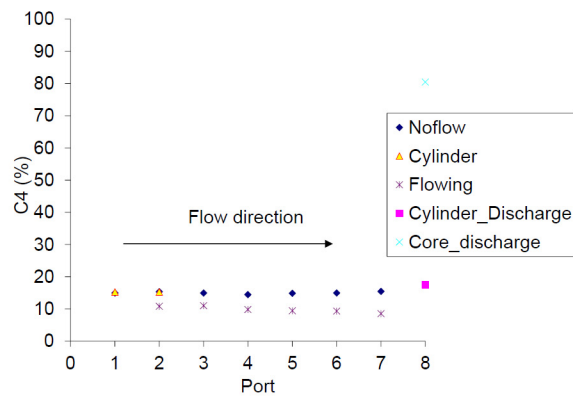
(b) Experiment 2

(c) Experiment 3

Figure 16—Mole fraction of C_4 in the following phase during capture experiments.

Compositional Variation in Gas-Condensate-Immobile Water Flow

Noncapture Experiments   Fig. 17 shows results of noncapture experiments for the case with immobile water in the core. Comparing results in Fig. 17 with results in Fig. 14 (without immobile water in the core), it is clear that in the presence of immobile water condensate still dropped out in the core. The compositional variation trend is the same as the case without immobile water.

(a) Experiment 1   (b) Experiment 2
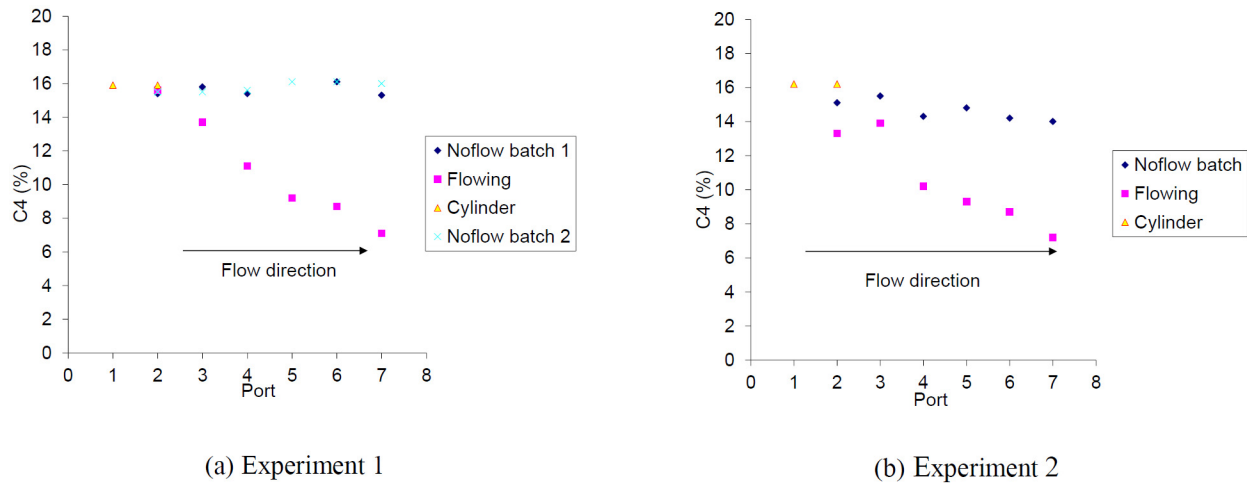
Figure 17—Mole fraction of C_4 in the following mixture during gas-condensate-immobile water noncapture experiment.

Capture Experiments Again, water did not have any significant effect on the compositional variation trend (Fig. 18). Condensate drop-outs were the same as in the two-phase case (Fig. 16). The nC_4 compositions of the discharge cylinder sample and core samples also increased, which further confirmed the accumulation of nC_4 in the condensate that had dropped out in the core.

(a) Experiment 1   (b) Experiment 2
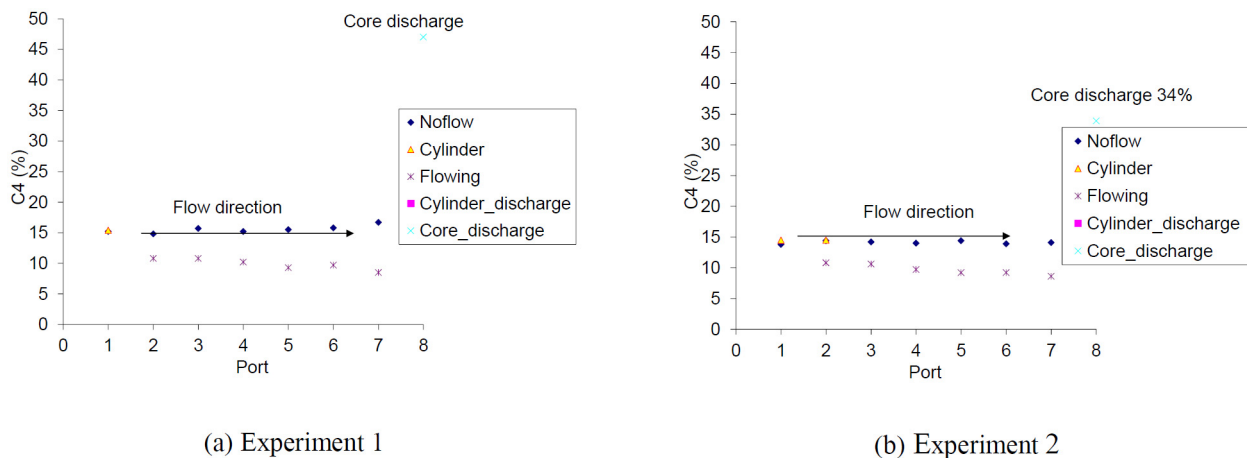
Figure 18—Mole fraction of C_4 in the following mixture during gas-condensate-immobile water capture experiment.

Saturation Profile

Fig. 19 shows condensate saturation distribution calculated from CT scanning together with the composition along the core from a noncapture experiment for gas-condensate system. The condensate saturation profile is consistent with the nC_4 compositional profile, although the saturation value estimated at slice #8 appears to be influenced by end-effect. It should be noted that due to the low porosity rock, there is only a small density difference between the liquid n-butane and methane, so the difference between CT numbers of C_1-nC_4 mixture saturated, C_1-saturated and nC_4-saturated rock is not large. This limits the accuracy of the saturation estimation. Nevertheless, the experimental results confirm the trend from simulation results in Fig. 6. Better accuracy of CT scanning may also be obtained with the aluminum instead of titanium core holder.
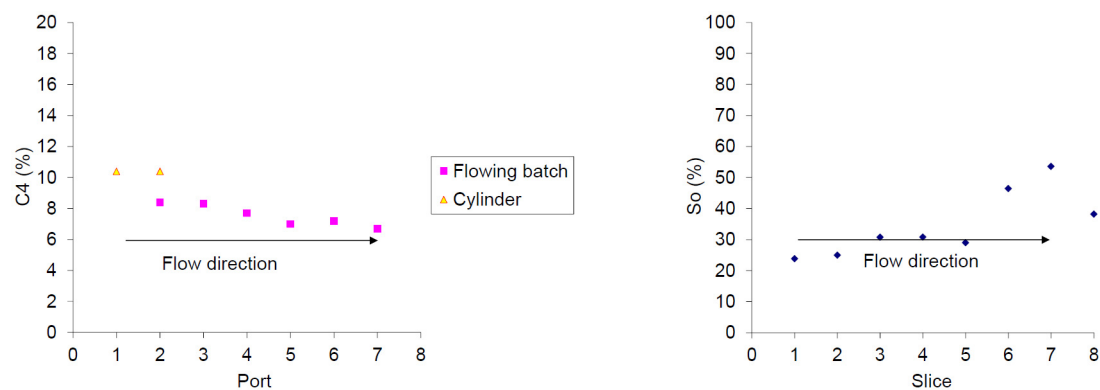
(a) nC_4 in the flowing phases   (b) Condensate saturation profile

Figure 19—Condensate saturation distribution from a noncapture experiment.

Conclusions

The main conclusions of this study are:

- Repeatability of the capture and noncapture experiments was achieved, demonstrating the validity of the results.
- Due to the relative permeability and the consequent difference in mobilities of gas and condensate phase, the local composition will change hence the phase envelope of the mixture will shift to the right. Reservoir fluid can be converted from gas condensate to volatile oil.
- Shutting a well to remove condensate bank may not be a good strategy as the condensate might not be able to revaporize due to the shift of the phase envelope.
- Condensate dropout can be reduced by minimizing the pressure drop below the dew point, either by producing the well slowly or by applying pressure maintenance.
- Condensate banking still occurs in the presence of immobile water. Immobile water did not have any measurable effect on the compositional variation of the gas condensate in the experiments performed here.

Acknowledgements

Nomenclature

Abbreviations

BHP	Bottom Hole Pressure
CCE	Constant Composition Expansion.
CT	Computerized Tomography
CVD	Constant Volume Depletion

Symbols

C_1	methane
C_4	butane
nC_4	n-butane (normal-butane)
CT_{cr}	CT number of condensate saturated rock

CT_{exp}	CT number of rock during experiments with C1-nC4 mixture
CT_{gr}	CT number of gas saturated rock
N_2	nitrogen
DI	De-Ionized
GC	Gas Chromatography
PLOT	Porous Layer Open Tubular
PVT	Pressure-Temperature-Volume
P_1	confining-pressure port
$P_2,\ldots,$	P_7 sampling ports
p_d	dew-point pressure
p_c	critical pressure
T_c	critical temperature
S_o	condensate saturation
S_{wi}	immobile water saturation

References

Afidick, D., Kaczorowski, N.J., and Bette, S. 1994. Production Performance of a Retrograde Gas Reservoir: A Case Study of the Arun Field. Presented at the SPE Asia Pacific Oil and Gas Conference, Melbourne, Australia, 7-10 November. SPE-28749-MS. http://dx.doi.org/10.2118/28749-MS.

Al Ismail, M.I. and Horne, R.N. 2014. An Investigation of Gas-Condensate Flow in Liquid-Rich Shales. Presented at the SPE Unconventional Resources Conference, the Woodlands, Texas, 1-3 April. SPE-169021-MS. http://dx.doi.org/10.2118/169021-MS.

Barnum, R.S., Brinkman, F.P., Richardson, T.W., and Spillette, A.G. 1995. Gas Condensate Reservoir Behavior: Productivity and Recovery Reduction Due to Condensation. Presented at the SPE Annual Technical Conference and Exhibition, Dallas, Texas, 22-25 October. SPE-30767-MS. http://dx.doi.org/10.2118/30767-MS.

Eilerts, C.K., Sumner E.F, and Potts N.L. 1965. Integration of Partial Differential Equation for Transient Radial Flow of Gas-Condensate Fluids in Porous Structures. *SPE Journal* **5**(02): 141–152. SPE-716-PA. http://dx.doi.org/10.2118/716-PA.

El-Banbi, A.H. and McCain W.D. 2000. Investigation of Well Productivity in Gas-Condensate Reservoirs. Presented at SPE/CERI Gas Technology Symposium, Calgary, Canada, 3-5 April. SPE-59773-MS. http://dx.doi.org/10.2118/59773-MS.

Fevang, Φ. and Whitson, C.H. 1996. Modeling Gas-Condensate Well Deliverability. *SPE Reservoir Engineering* **11**(04): 221–230. SPE-30714-PA. http://dx.doi.org/10.2118/30714-PA.

Fussell, D.D. 1973. Single-Well Performance Predictions for Gas Condensate Reservoirs. *JPT* **25**(07): 860–870. SPE-4072-PA. http://dx.doi.org/10.2118/4072-PA.

Izuwa, N.C., Obah, B., and Appah, D. 2014. Optimal Gas Production Design in Gas Condensate Reservoir. Presented at the SPE Nigeria Annual International Conference and Exhibition, Lagos, Nigeria, 5-7 August. SPE-172453-MS. http://dx.doi.org/10.2118/172453-MS.

Jones, J.R. and Raghavan, R. 1988. Interpretation of Flowing Well Responses in Gas-Condensate Wells. *SPE Formation Evaluation* **3**(03): 578–594. SPE-14204-PA. http://dx.doi.org/10.2118/14204-PA.

Jones, J.R., Vo, D.T., and Raghavan, R. 1986. Interpretation of Pressure Buildup Responses in Gas-Condensate Wells. *SPE Formation Evaluation* **4**(01): 93–104. SPE-15535-PA. http://dx.doi.org/10.2118/15535-PA.

Kniazeff, V.J. and Naville, S.A. 1965. Two-Phase Flow of Volatile Hydrocarbons. *SPE Journal* **5**(01). SPE-962-PA. http://dx.doi.org/10.2118/962-PA.

Muskat, M. 1949. *Physical Principles of Oil Production,* first edition. New York: McGraw-Hill Book Co.

Novosad, Z. 1996. Compositional and Phase Changes in Testing and Producing Retrograde Gas Wells. *SPE Reservoir Engineering* **11**(04): 231–235. SPE-35645-PA. http://dx.doi.org/10.2118/35645-PA.

O'Dell, H.G. and Miller, R.N. 1967. Successfully Cycling a Low Permeability, High-Yield Gas-Condensate Reservoir. *JPT* **19**(01): 41–47. SPE-1495-PA. http://dx.doi.org/10.2118/1495-PA.

Roebuck, I.F., Henderson, G.E., Doughlas, J., and Ford, W.T. 1968a. The Compositional Reservoir Simulator: Case I –The Linear Model. *SPE Journal* **9**(01): 115–130. SPE-2033-PA. http://dx.doi.org/10.2118/2033-PA.

Roebuck, I.F., Ford, W.T., Henderson, G.E., and Doughlas, J. 1968b. The Compositional Reservoir Simulator; Case IV –The Two Dimensional Model. *Presented at the SPE Annual Fall Meeting,* Houston, Texas, 29 September-2 October. SPE 2235-MS. http://dx.doi.org/10.2118/2235-MS.

Roussennac, B. 2001. *Gas Condensate Well Test Analysis*. M.S. Thesis, Stanford University, Stanford, California (2001).

Seah, Y.H., Gringarten, A.C., Giddins, M.A., and Burton, K. 2014. Optimising Recovery in Gas Condensate Reservoirs. Presented at the SPE Asia Pacific Oil and Gas Conference, Adelaide, Australia, 14-16 October. SPE-171519-MS. http://dx.doi.org/10.2118/171519-MS.

Shi, C., Horne, R.N., and Li, K. 2006. Optimizing the Productivity of Gas/Condensate Wells. Presented at the SPE Annual Technical Conference and Exhibition, San Antonio, Texas, 24-27 September. SPE 103255-MS. http://dx.doi.org/10.2118/103255-MS.

Shi, C. and Horne, R.N. 2008. Improved Recovery in Gas-Condensate Reservoir Considering Compositional Variations. Presented at the SPE Annual Technical Conference and Exhibition, Denver, Colorado, USA, 21-24 September. SPE-15786-MS. http://dx.doi.org/10.2118/115786-MS.

Shi, C. 2009. *Flow Behaviors of Gas Condensate Wells*. Ph.D. Dissertation, Stanford University, Stanford, California (March 2009).

Siddiqui, M.A.Q., Al-Nuaim, S., and Khan, R.A. 2014. Stochastic Optimization of Gas Cycling in Gas Condensate Reservoirs. Presented at the Abu Dhabi International Petroleum Exhibition and Conference, Abu Dhabi, UAE, 10-13 November. SPE-172107-MS. http://dx.doi.org/10.2118/172107-MS.

Siddiqui, M.A.Q., Al-Nuaim, S., and Khan, R.A. 2015. Well Placement and Rate Optimization for Gas Cycling in Gas Condensate Reservoirs. SPE Middle East Oil & Gas Show and Conference, Manama, Bahrain, 8-11 March. SPE-172641-MS. http://dx.doi.org/10.2118/172641-MS.

Vo, H. X. 2010. *Composition Variation During Flow of Gas-Condensate Wells*. M.S. Thesis, Stanford University, Stanford, California (2010).

Zhang, H.R. and Wheaton, R.J. 2000. Condensate Banking Dynamics in Gas Condensate Fields: Compositional Changes and Condensate Accumulation around Production Wells. Presented at the SPE Annual Technical Conference and Exhibition, Dallas, Texas, 1-4 October. SPE-62930-MS. http://dx.doi.org/10.2118/62930-MS.